Proceedings of ASME Turbo Expo 2004
Power for Land, Sea, and Air
June 14-17, 2004, Vienna, Austria

GT2004-53882

TIP LEAKAGE / MAIN FLOW INTERACTIONS IN MULTI-STAGE HP TURBINES WITH SHORT-HEIGHT BLADING

Piotr Lampart
Institute of Fluid Flow Machinery
Polish Academy of Sciences, Gdańsk, Poland

Sergey Yershov, Andrey Rusanov
Institute of Mechanical Engineering Problems
Ukrainian Academy of Sciences, Kharkov, Ukraine

Mariusz Szymaniak
Institute of Fluid Flow Machinery
Polish Academy of Sciences, Gdańsk, Poland

ABSTRACT

Interaction of the main flow with tip leakage over shrouded rotor blades in a multi-stage turbine is studied numerically. The flow in blade-to-blade channels is computed with the aid of a 3D Navier-Stokes solver FlowER with the Menter SST turbulence model. In this paper, the labyrinth seals are not computed but the numerical scheme is modified to include the source/sink-type boundary conditions at places at the endwalls referring to design locations of injection of leakage flows into, or their extraction from, the blade-to-blade passage. Without considering complete labyrinth seal geometries, the tip leakage jet is represented by its flow rate and direction at re-entry to the blade-to-blade passage, as if referring to the performance of a range of different labyrinth seal arrangements. The effect of direction of tip leakage re-entry on the downstream flow and efficiency of the turbine stage (stage group) is studied. The calculation method is validated on a model air stator/rotor turbine.

INTRODUCTION

Tip leakage gives rise to losses of work in a turbine stage rotor, but its energy is still available for work in the subsequent turbine stage. Typically, tip leakage flow at re-entry to the blade-to-blade passage has different parameters as compared to the main stream. The most important is the difference between the velocities in the tip leakage and in the main flow, which results in downstream mixing and enthalpy losses. As shown by Denton [1], the enthalpy losses tend to remain proportional to the relative leakage flow rate. A simple model of mixing of two streams assumed in [1] shows that the proportionality factor depends on the direction of the tip leakage jet at its re-entry downstream of the turbine rotor, as related to the direction of the main stream there. However, small axial gaps between the turbine stages usually do not allow for the mixing process to be accomplished in the stage where it is originated. There will also be an off-design inflow onto the downstream stator blade at the tip, with possible pressure-side separation and changes in location of laminar-turbulent transition.

Tip leakage as a mass extraction and injection also interacts with endwall flows, see Hunter & Manwaring [2], Giboni et al. [3], Lampart et al. [4]. As shown in [4], tip leakage can reduce the span-wise extension of secondary flow zones (and reduce secondary flow losses) by sucking out the high-entropy boundary layer fluid into the labyrinth seals. Leakage flows as mass deficits in the blade-to-blade passages can also increase the risk of separation or extend the separation zone.

Great efforts have been made recently to reduce tip leakage losses in conventional labyrinth seals. A considerable reduction of leakage flow rate can be achieved by application of brush seals, see Bayley and Long [5], Stephen and Hogg [6]. Another approach to redesign of labyrinth seals, using special turning devices, or bladelets, installed on the shrouds is presented by Wallis et al. [7]. This design enables changing the tip leakage jet swirl angle with the aim to reduce losses of downstream mixing of the tip leakage with the main stream. The possibility of changing the tip leakage swirl velocity and swirl angle using shroud bladelets is also shown in a CFD study of Lampart & Szymaniak [8]. While sample patterns of velocity magnitude and circumferential component of the velocity for two types of labyrinth seals – a classical labyrinth seal and a labyrinth seal with shroud bladelets – found in [8] are illustrated in Fig. 1, it is still not clear how bladelets quantitatively reduce the tip leakage losses and increase the efficiency of the stage (stage group).

3D modelling of flow in the entire impulse turbine stage or a group of stages with side flow passages, including tip leakage over shrouded rotor blades, leakage through stator seals, leakage through rotor disc holes, and windage flows in passages between the fixed and rotating parts of the machinery, still remains an extremely difficult task. The main difficulty lies in the complexity of turbomachinery geometries, and different aspect ratios, flow scales and periodicity between the main flow in the blade-to-blade passages and side flows. Computational resources needed to fulfil basic CFD principles on grid refinements of the flow domain are very large. While a number of 3D CFD computations of stator/rotor passages with shroud cavities are reported in the literature, see Gier et all. [9] Anker & Mayer [10], Lampart & Szymaniak [8] (all single blade-to-blade passage computations assumming axisymmetric flow patterns, with reference [9] also giving a detailed quantitative breakdown of cavity-related losses), the authors of this paper still find it not easy to quantitatively evaluate the efficiency of different labyrinth seal designs from such computations.

Therefore, another approach to investigation of loss mechanisms and flow efficiency will be pursued. In this paper, we will not discuss particular designs of tip leakage labyrinth seals, nor calculate labyrinth seal geometries. 3D flow in the blade-to-blade channels will be investigated and the performance of various labyrinth seals will be represented in the form of a jet leaving and re-entering the blade-to-blade passage, characterised by its mass flow rate and direction at re-entry. The effect of tip leakage mass flow rate and direction on the downstream flow and turbine efficiency will be studied.

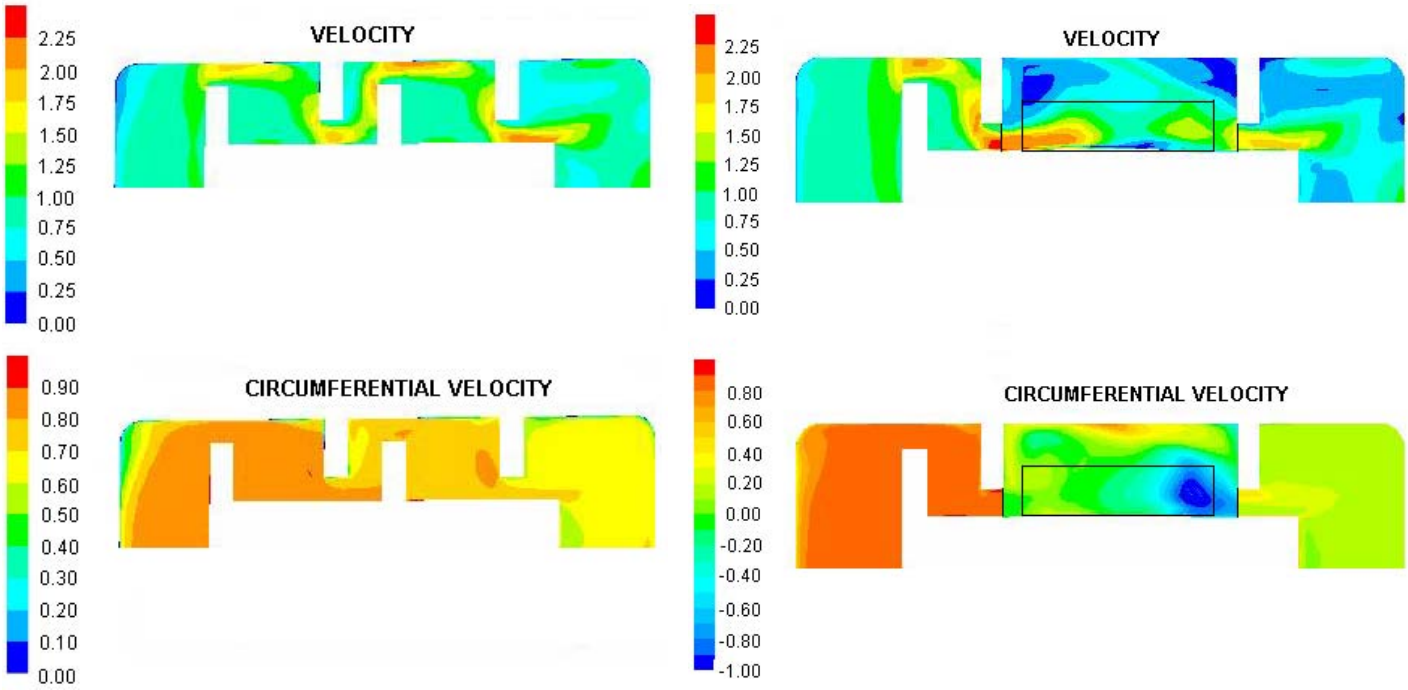

Fig. 1. Velocity magnitude and circumferetial component of the velocity for a classical labyrinth seal (left) and a labyrinth seal with shroud bladelets (right)*.

*Velocities are non-dimensional with respect to the inlet velocity. In the right picture velocities in the bladelet region are plotted in the rotating reference frame; black lines indicate the location of bladelets and interface planes between the fixed and rotating computational domains. The computations were made in FLUENT using a segregated solver.

FLOW MODEL

The analysis presented in this paper is based on numerical investigations carried out with the help of a CFD RANS-based code FlowER - solver of viscous (turbulent), compressible flow in turbomachinery environment, see Yershov & Rusanov [11], Yershov et al. [12]. The effects of turbulence are taken into account using the k-ω SST model. The governing equations are solved numerically based on the Godunov-type upwind differencing, high-resolution ENO scheme and implicit operator δ (characteristic variables are used), assuring second-order accuracy everywhere in space and time. Multi-stage computations are carried out in one blade-to-blade passage of the stator and rotor from each stage of a calculated stage group. The computations converge to a steady state, with the assumed condition of spatial periodicity, and mixing plane approach between the fixed and rotating domains. The inlet/exit boundary conditions impose the pressure drop and let the mass flow rate be resultant.

The flow is solved only in blade-to-blade passages, while leakage flows are simulated in the form of extracted and injected jets. The computational domain is modified at the endwalls where some places are permeable boundaries of the domain - sources or sinks, see Fig. 2. In addition to the boundary conditions typical for turbomachinery codes, source/sink-type boundary conditions are used at places at the endwalls referring to design locations of injection of leakage and windage flows into, or their extraction from, the blade-to-blade passage. For extractions (sinks), one boundary condition is needed - mass flow rate. For injections (sources), there are four boundary conditions – mass flow rate, total temperature, meridional and swirl angle, recalculated into boundary values of characteristic variables. The above approach embodies the message that although leakage flow rates are inherent to labyrinth seal or passage geometries, most of entropy creation due to leakage flows takes place not in the labyrinth seals or leakage flow passages, but in the blade-to-blade passage downstream of the leakage jet re-entry where the injected leakage jet mixes with the main stream, Denton [1].

In this study source/sink gaps belong to the rotor domain, so the source/sink terms are resolved in the rotating reference frame. The mass flow rate condition is formulated to be satisfied integrally through each orifice, and is allowed to vary from node to node of the orifice. The distribution of mass flow rate in the orifice is affected by stream-wise and pitch-wise gradient of static pressure in the rotor near the endwalls. The velocity

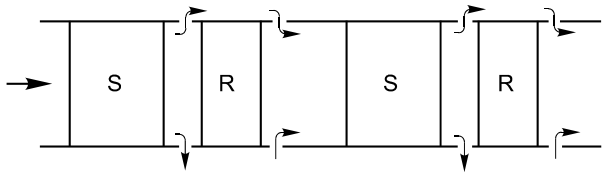

Fig. 2. Computational domain with source/sink-type boundaries; S - stator, R - rotor.

components at the source orifice are calculated based on the constant total pressure, input flow angles and size of the orifice.

The presented method enables computation of interaction of the leakage flows with the main stream, secondary flows, separations and other phenomena. Mass averaged kinetic energy losses of a stage can be found from a formula that takes into account leakage streams

$$\xi = \sum_{ex.+s.} \xi_i G_i \,/\, \sum_{ex.+s.} G_i$$

where the summation extends on all streams that carry away the fluid from the blading system (exit and sinks) and ξ_i is the kinetic energy loss, G_i - mass flow rate in a stream i. In the case of nominal directions of leakages and equal intensities of respective sources and sinks, and with the assumption of no enthalpy loss between the sink and source jets, the formula reduces to the summation over exit streams only. Exit energy losses can be found as in non-source/sink computations.

MODEL AIR TURBINE STAGE - COMPARISON OF EXPERIMENTAL AND COMPUTATIONAL RESULTS

In the course of investigations, the presented approach is validated on a model air turbine stage of the Institute of Thermal Engineering (ITC) Łódź, Poland - model TK9-TW3. This turbine tested experimentally by Wiechowski [13] has a geometry of typical low-load HP impulse turbine stages, with shrouded stator and rotor blades and typical labyrinth seals. It operates with short-height cylindrical blading and aft-loaded stator profiles of aspect ratios: span/chord - 0.73 (stator) and 2.20 (rotor), pitch/chord - 0.86 (stator) and 0.80 (rotor), span/diameter - 0.08 (stator and rotor). The thermodynamic conditions are: pressure drop from 1 to 0.9 bar, inlet temperature - 320K, average reaction - 0.23 (nominal conditions), mass flow rate - 4.0 kg/s (nominal conditions). The experimental data are available for a wide range of operating conditions u/c_{0T} between 0.3 and 0.9 (u - rotor speed at the mid-span, c_{0T} – velocity based on theoretical enthalpy drop across the stage), achieved by changing the rotor rotational speed. The computations are carried out for three values of u/c_{0T} equal to 0.45, 0.54 (nominal conditions) and 0.65. A uniform profile of total pressure and low level of free-stream turbulence are assumed at the inlet. The computations are made on an H-type grid of 1000000 cells - 88x76x72 (axially, spanwise and pitch-wise) in the stator + 96x76x72 in the rotor. The grid is refined near the endwalls and blade walls, also near the trailing and leading edges, see Fig. 3. Grid refinement at the walls fulfils requirements of the assumed turbulence model (y^+=2). The grid was chosen so as to minimise both the grid size and grid dependence, relying on the observation that the obtained results showed no visible change in flow patterns nor any change in stage efficiency, as compared to those on a more refined grid of 1200000 cells.

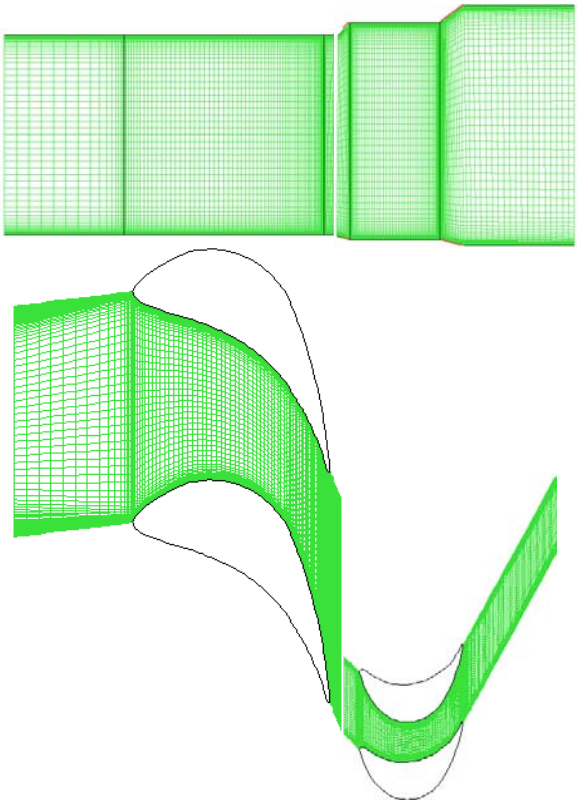

Fig. 3. Model air turbine – computational grids for the stator and rotor cascades in meridional view (top), and blade-to-blade section (bottom).

The computations were carried out first without considering leakage flows (source/sink slots closed), and then with leakage both at the root and tip (source/sink slots open). In the latter case prior to CFD computations, the stage was calculated using a complex of 0D/1D procedures to estimate the mass flow rates of the main flow in the blade-to-blade passage of the stator and rotor G_1, G_2 as well as flow rates of leakages at the tip and root G_T, G_R and windage flows G_W, $G_{W'}$ based on the given pressure drops and geometry of labyrinth seals and passages, see Gardzilewicz [14]. The obtained leakage flow rates necessary for further 3D computations are as follows: $G_T=1.2\%G_1$, $G_W=G_{W'}=0.6\%G_1$. It was assumed that leakage jets re-enter the blade-to-blade passage normal to the source slots in the meridional plane, that is at an angle -55° at the tip and 75° at the root - measured clockwise from the projection of the turbine axis at the meridional plane. The swirl angle of the tip leakage jet was assumed 75° - measured clockwise from the projection of the turbine axis on the blade-to-blade plane (the swirl angle of the tip leakage jet is that of the main stream downstream of the stator, assuming no change in the labyrinth seal). Due to lack of further information on the mean direction of the root leakage jet, it was injected at a swirl angle of 60°.

Fig. 3 shows a comparison of experimental data and computational results (both without and with leakage flows) downstream of the rotor. The comparison includes axial velocity, absolute swirl velocity, absolute velocity and absolute swirl angle (measured clockwise from the projection of the turbine axis on the blade-to-blade plane) for three operating conditions - u/c_{0T}=0.45 (off-design), 0.54 (nominal) and 0.65 (off-design). The computed distributions were captured at a section located 135% of the axial chord downstream of the rotor trailing edge, that is at a distance corresponding to the location of the measuring probe at the experimental facility. The reference axial section is relatively far downstream of the blading system, therefore, it is expected that the processes of mixing and dissipation of 3D flow structures are largely accomplished there. This is why the experimental and computational distributions of the investigated quantities do not exhibit considerable secondary flow peaks characteristic for sections more upstream. In general, the computational and experimental results reveal satisfactory qualitative and also quantitative agreement for the three investigated values of load. The span-wise locations of the largely dissipated secondary flow peaks are reproduced relatively well in the computational results.

There are some discrepancies between the computational and experimental results at the root and tip sections, for the presented three operating conditions (let us note that for off-design conditions, an increased swirl velocity and swirl angle downstream of the rotor is observed, which can either increase the leaving loss or deteriorate inflow conditions at the subsequent blade row). Understandably, the computations without leakages underestimate the absolute swirl velocity and swirl angle near the endwalls. In real situation, the unturned tip leakage stream with the large circumferential component of the velocity, hardly changed through the labyrinth seal as compared to that downstream of the stator, gives rise to an increased swirl velocity and swirl angle near the tip. This can also be seen from computations with leakage flows. The computations with leakage flows better agree with the experimental data, but seem to slightly overestimate the swirl velocity and swirl angle near the endwalls. It is still possible that the real mean swirl angles of the leakage jets at the root and tip at reentry to the blade-to-blade passage were smaller in the experiment than those assumed for the computations (75° for the tip leakage jet and 60° for the root leakage jet), thus introducing in reality less momentum at the endwalls in circumferential direction.

More examples of validation of the flow solver on turbomachinery test cases, including Durham low speed turbine cascade, NASA Rotor37 and NASA low speed centrifugal compressor can be found in Lampart et al. [15].

EFFECT OF TIP LEAKAGE FLOW RATE AND DIRECTION IN A TWO-STAGE TURBINE GROUP

Interaction of the tip leakage with the main flow is investigated on a two-stage group of an HP impulse turbine with short-height cylindrical blading. Root leakages are neglected in

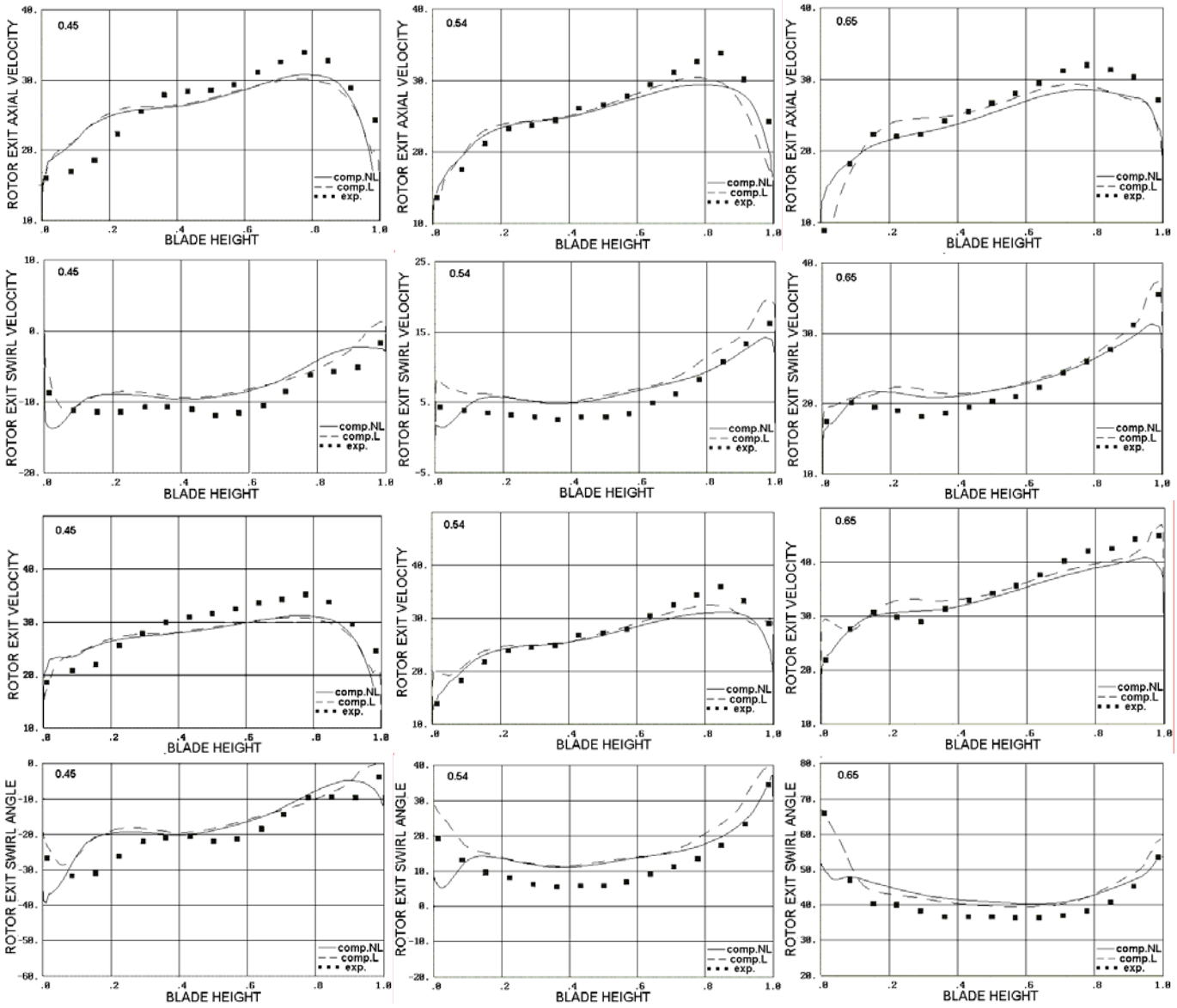

Fig. 4. Model air turbine - computed and experimental axial velocity (top), absolute swirl velocity (top centre), absolute velocity (bottom centre) and absolute swirl angle (bottom) at the rotor exit: u/c_{0T}=0.45 (left), 0.54 (centre), 0.65 (right);
comp.NL – computed without leakages, comp.L – computed with root and tip leakages, exp. – experimental.

this investigation. Basic dimensions of the blading systems are: span/chord - 0.75 (stator) and 2.00 (rotor), pitch/chord - 0.75 (stator and rotor). The thermodynamic conditions assumed for the investigation are: pressure drop from 88 to 70 bar, inlet temperature - 760K. The mass flow rate for these conditions and geometry is 170.0 kg/s, average reaction - 0.2. The assumed conditions are "slightly off-design" – pressure drop 10% below that of nominal conditions. The tip leakage mass flow rate is varied during the investigation from 1% up to 4% of the flow rate in the blade-to-blade passage of the stator cascade. The swirl angle of the leakage jet at re-entry is varied from 0^o to 80^o (measured clockwise from the projection of the turbine axis on the blade-to-blade plane). Let us note that a typical swirl angle of the tip leakage jet for impulse turbines with classical labyrinth seals can be assumed equal to the swirl angle of the main stream downstream of the stator cascade, that is about 78^o in our case. The meridional angle of the tip leakage jet is varied from -90^o to -30^o (measured clockwise from the projection of the turbine axis on the meridional plane). The angle -90^o means no axial velocity at re-entry to the blade-to-blade passage (tip leakage jet is directed radially inwards).

Tip leakage has an effect on flow in the rotor where it is originated (first rotor), as well as in subsequent blade rows. Changes in the rotor depend on the leakage flow rate. Tip leak-

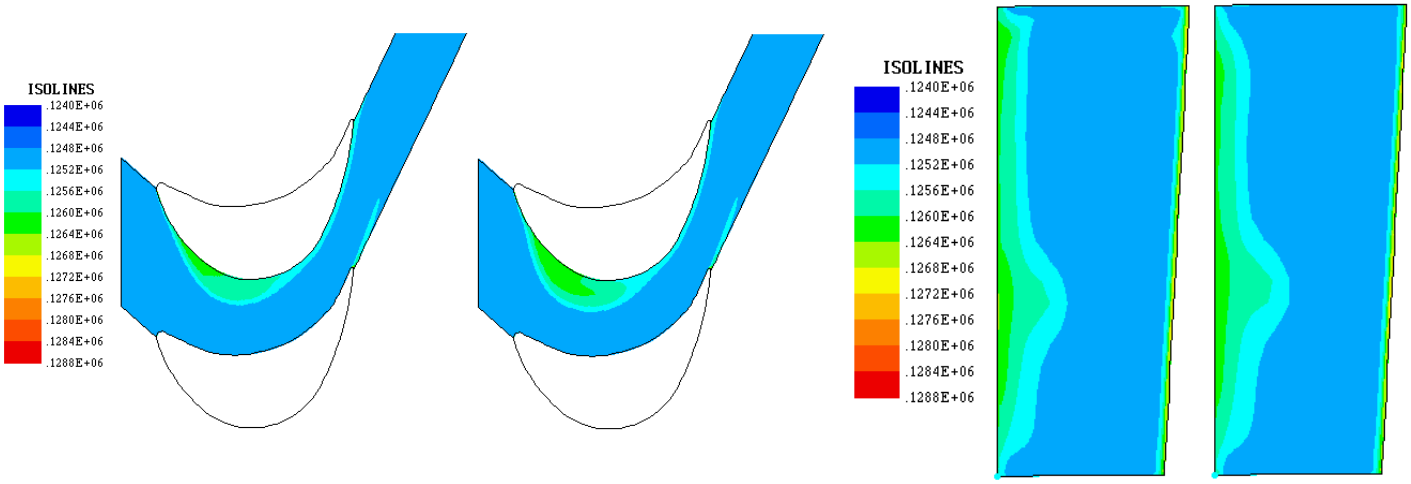

Fig. 5. Entropy function contours in the blade-to-blade plane of the first rotor 10% blade height from the hub (left) and in the normal plane at the rotor trailing edge (right) for leakage mass flow rate 1% (left) and 3% (right).

age flow acts here as a mass deficit for the blade-to-blade passage. The mean axial velocity is reduced, which may locally increase the incidence angle. This effect can be observed from the right hand side of Fig. 5 showing entropy function contours in the first rotor 10% of the blade height from the hub for two leakage flow rates 1% and 3% (of the stator mass flow rate). Due to the increased incidence at the rotor there, the size of the separation zone increases with the increasing leakage flow rate, thus increasing separation losses for these "slightly" off-design conditions (the separation takes place up to 35-40% blade span from the hub). On the other hand, tip leakage flow helps to remove tip boundary layer fluid from the blade-to-blade passage upstream of the rotor, which retards the development of secondary flows at the tip. It is shown in the right-hand side of Fig. 5 giving entropy function contours in the normal plane at the rotor trailing edge for the two leakage flow rates that the extension of secondary flow zone at the tip is decreased, thus decreasing the secondary flow losses, with the increasing leakage flow rate.

Changes in the downstream stator depend both on the leakage flow rate and its direction at re-entry to the blade-to-blade passage. Fig. 6 shows the absolute swirl velocity at the rotor exit measured 75% of the axial chord downstream of the rotor trailing edge, for three directions of tip leakage jet re-entry. The swirl velocity in the tip region is seen to increase largely above the mid-span value, with the increasing swirl angle of the tip leakage jet. Therefore, for large swirl angles of the tip leakage jet, more downstream mixing can be expected along with an off-design inflow onto the downstream stator blade. This off-design inflow can be observed from Fig. 7 showing velocity vectors in the second stator 8% of the blade height from the tip for two directions of tip leakage jet re-entry – tip leakage swirl angle 0^o and 80^o.

Due to the fact that the tip leakage suppresses the secondary flow at the tip in the rotor, no recirculating flow typical for secondary flow is observed at the tip downstream of the rotor. The typical structure downstream of re-entry of the leakage jet is that of mixing of two streams - under conditions of positive pressure gradient and in the vicinity of the stationary wall. But the recirculating flow will be enhanced in the second stator at the tip. The off-design inflow for a large swirl angle of the leakage jet will increase profile losses in the tip region, and also increase secondary flow losses due to the intensified cross flow in the blade-to-blade passage. The direction of tip leakage jet re-entry has a considerable effect on re-circulating flow in the tip region of the downstream stator. Fig. 8 shows the comparison of entropy function contours in the normal plane downstream of the second stator, first comparing the results for two tip leakage jet flow rates 1% and 3% (at a tip leakage jet swirl angle 0^o), and then for three swirl angles 40^o, 60^o and 80^o (at a 3% tip leakage mass flow rate). It is clear from the figure that the loss centre of recirculating fluid moves towards the mid-span and the overall level of losses increases with the increasing tip leakage jet flow rate and swirl angle.

Enthalpy losses in subsequent blade rows of the calculated configuration of a two-stage HP impulse turbine are quantified to evaluate changes of losses with the changing tip leakage jet mass flow rate and direction at re-entry. Fig. 9 shows sample graphs of enthalpy losses in the first stator, rotor and stage, as well as second stator, second rotor and stage, obtained as a function of tip leakage jet swirl angle - ranging from 0^o to 80^o, for two mass flow rates of the tip leakage – 1% and 3%, and three meridional angles of the tip leakage jet at re-entry -90^o (directed radially inwards), -60^o and -30^o. Expressions used to calculate stator, rotor and stage losses are enclosed in Appendix. The presented stage losses do not include exit energy losses. Note that losses of subsequent blade rows are captured at respective mixing (exit) planes which for stators are located 10% of the stator axial chord downstream of the stator trailing

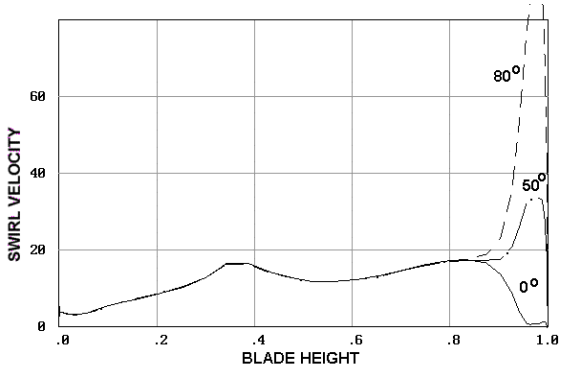

Fig. 6. Absolute swirl velocity at the rotor exit for three values of tip leakage jet swirl angle 0°, 50° and 80°; leakage flow rate 3%, meridional angle –90°.

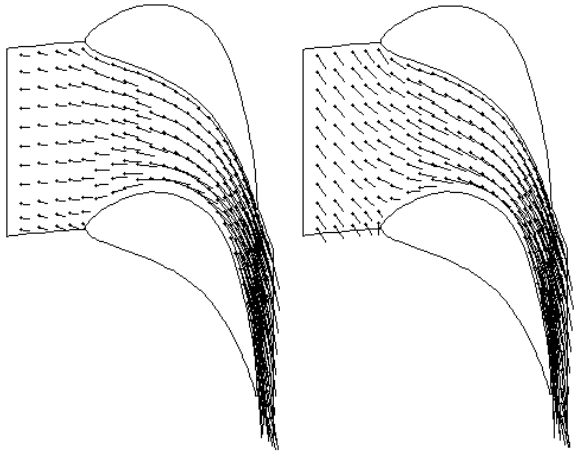

Fig. 7. Velocity vectors in the second stator 8% blade height from the tip for the tip leakage jet swirl angle 0° (left) and 80° (right); leakage flow rate 3%, meridional angle –90°.

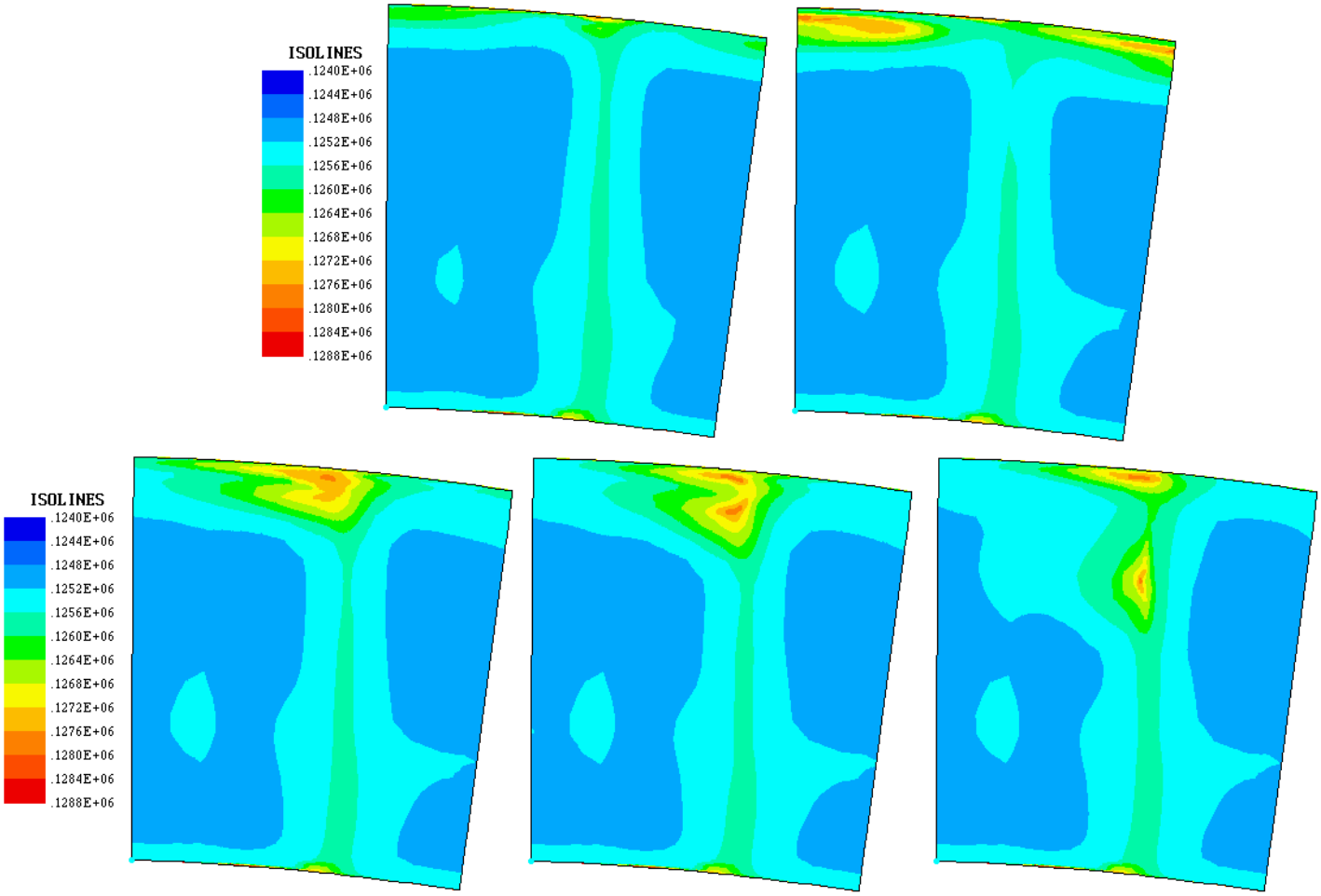

Fig. 8. Entropy function contours in the normal plane downstream of the second stator: tip leakage jet flow rate 1% and 3%; swirl angle 0°, meridional angle –90° (top); tip leakage jet flow rate 3%; swirl angle 40°, 60° and 80°, meridional angle –90° (bottom).

edge, for rotors (and stages) 75% of the rotor axial chord downstream of the rotor trailing a section rotor and stage losses are captured at a section located 75% of the rotor axial chord downstream of the rotor trailing edge. The computed flow losses in subsequent blade rows exhibit an increasing tendency with the increasing mass flow rate of the tip leakage. Flow losses also increase with the increasing tip leakage jet swirl angle. Due to the fact that the circumferential velocity of the main stream has some positive value at the rotor exit (see Fig. 6) for this system of stages, the computed minimum of enthalpy losses with respect to swirl angle is located between 0^o and 20^o. If the leakage jet swirl angle is increased from this value up to 80^o, the enthalpy losses in the stage may increase by almost 1.5% (for a large leakage flow rate 3%), the loss increase coming both from the rotor where the tip leakage is formed, and from subsequent stator and rotor cascades.

CONCLUSIONS

Investigations of the effect of tip leakage over shrouded rotor blades were carried out in a multi-stage configuration, using a source/sink approach. The performance of various labyrinth seals was represented here in the form of a jet leaving and re-entering the blade-to-blade passage, characterised by its mass flow rate and direction at re-entry. A two-stage turbine at "slightly" off-design conditions was investigated and the effect of tip leakage flow rate and direction was scrutinised downstream of the first rotor, second stator and second rotor.

It was found that the tip leakage interacts with the main flow and endwall flows of the blade row where it is originated. It intensifies the recirculating flow at the tip endwall of the downstream stator, and also affects the downstream rotor. For large tip leakage flow rates, reducing the tip leakage swirl an gle was found to bring up to a 1.5% decrease in enthalpy losses

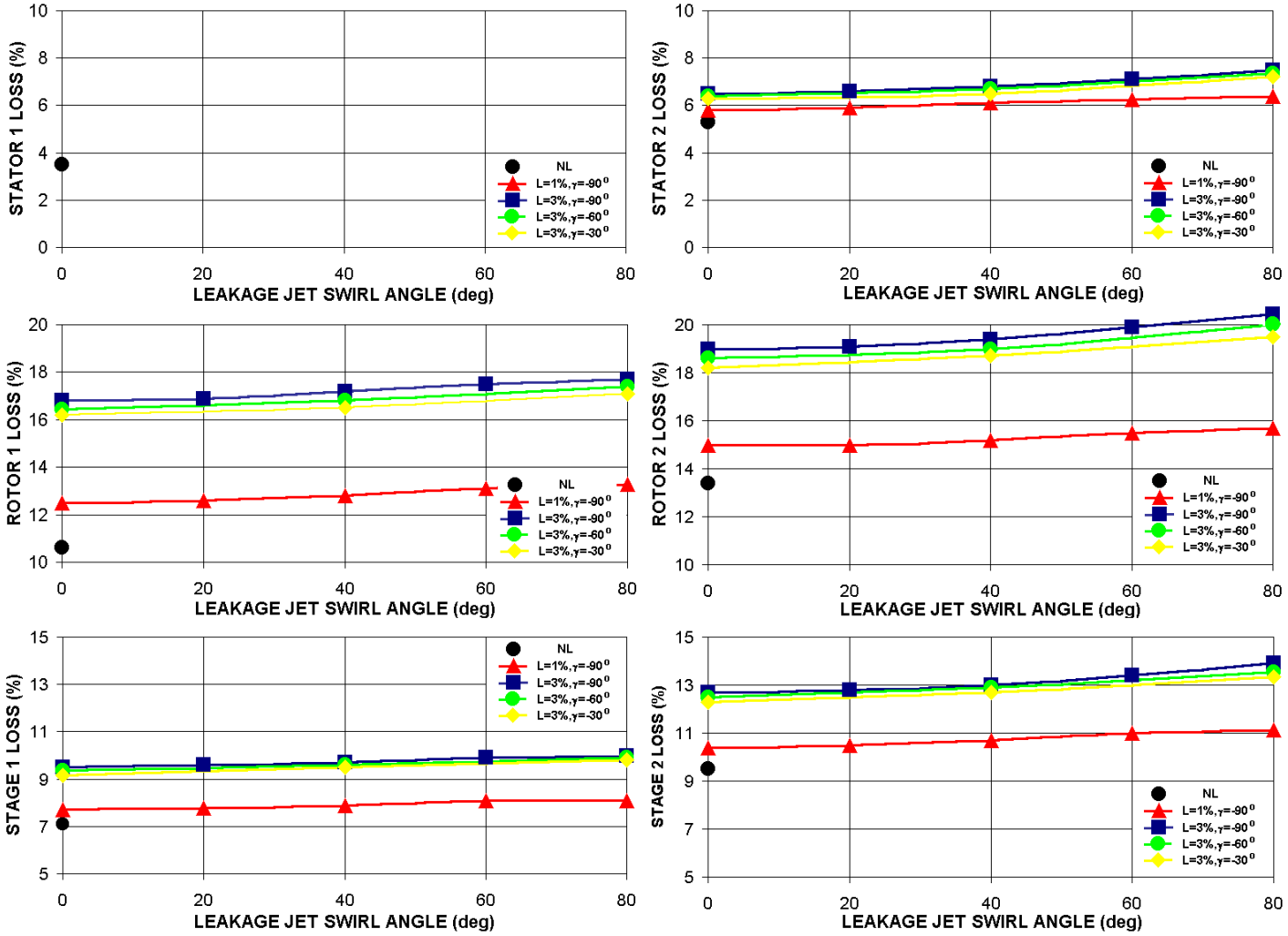

Fig. 9. Mass averaged enthalpy losses in the first stator, rotor and stage (left), second stator, rotor and stage (right) as a function of tip leakage jet swirl angle at re-entry for two leakage flow rates of 1% or 3% and three leakage jet meridional angles -90^o, -60^o, -30^o. Computational results without leakage are indicated by a black circle. Enthalpy losses in the first stator do not change when the leakage is modelled.

of the stage. Therefore, further efforts to design labyrinth seals changing the leakage jet swirl angle may turn out beneficial.

REFERENCES

[1] Denton J.D., 1993, Loss mechanisms in turbomachines, ASME J. Turbomachinery, Vol.115.

[2] Hunter S.D., Manwaring S.R., 2000, Endwall cavity flow effects on gaspath aerodynamics in an axial flow turbine, Part I – Experimental and numerical investigations, ASME Pap. 2000-GT-651. Part II – Source term model development, ASME Pap. 2000-GT-513.

[3] Gibboni A., Menter J.R., Peters P., Wolter K., Pfost H., Breisig V., 2003, Interaction of labyrinth seal leakage flow and main flow in an axial turbine, ASME Pap. GT2003-38722.

[4] Lampart P., Gardzilewicz A., Yershov S., Rusanov A., 2000, Investigation of flow characteristics of an HP turbine stage including the effect of tip leakage and windage flows using a 3D Navier-Stokes solver with source/sink-type boundary conditions, ASME Pap. IJPGC 2000-15004.

[5] Bayley F.J., Long C.A., 1993, A combined experimental and theoretical study of flow and pressure distribution in a brush seal, Trans. ASME, J. Eng. Gas Turbines Power, Vol. 115.

[6] Stephen D., Hogg S., 2003, Development of brush seal technology for steam retrofit applications, ASME Pap. IJPGC 2003-40103.

[7] Wallis A.M., Denton J.D., Demargne A.A.J., 2000, The control of shroud leakage flows to reduce aerodynamic losses in a low aspect ratio shrouded axial flow turbine, ASME Pap. 2000-GT-475.

[8] Lampart P., Szymaniak M., 2004, CFD study of turbine labyrinth seals with shroud bladelets, Rep. Institute of Fluid Flow Machinery 3848/03.

[9] Gier J., Stubert B., Brouillet B., de Vito L., 2003, Interaction of shroud leakage flow and main flow in a three-stage LP turbine, ASME Pap. GT2003-38025.

[10] Anker J.E., Mayer J.F., 2001, Computational study of the interaction of labyrinth seal leakage flow and main flow in an axial turbine, Proc. 4th European Conference on Turbomachinery Fluid Dynamic and Thermodynamics, Florence, Italy, March 18-23, pp. 639-653.

[11] Yershov S., Rusanov A., 1996, The application package FlowER for the calculation of 3D viscous flows through multistage turbomachinery, Certificate of Ukrainian state agency of copyright and related rights, Kiev, Ukraine, February 19.

[12] Yershov S., Rusanov A., Gardzilewicz A., Lampart P., Świrydczuk J., 1998, Numerical simulation of viscous compressible flows in axial turbomachinery, TASK Quarterly, Vol. 2, No. 2, pp. 319-347.

[13] Wiechowski S., 1988, Results of investigations of annular cascades TK8, TK9 and models TK8-TW3, TK9-TW3, Rep. Inst. Thermal Engng. (in Polish).

[14] Gardzilewicz A., 1984, Selected problems of computer-aided design of steam turbines and heat cycles, Rep. Inst. Fluid Flow Machinery 161/84 (in Polish).

[15] Lampart P., Yershov S., Rusanov A., 2002, Validation of turbomachinery flow solver on turbomachinery test cases, Turbomachinery, Vol. 122, pp. 63-70.

APPENDIX

In this appendix, enthalpy losses in the stator, rotor and stage are defined. The definitions are gathered in Tab. 1 and are easily explained with the help of Fig. 10 showing an enthalpy-entropy diagram of the expansion process in a turbine stage.

Stator loss	$\xi_1 = (h_1 - h_{1s}) / (h_{0T} - h_{1s})$
Rotor loss	$\xi_2 = (h_2 - h_{2s}) / (h_{1T} - h_{2s})$
Stage loss (without exit energy = stator + rotor loss)	$\xi_{12} = (h_2 - h_{2s'}) / (h_{0T} - h_{2s'})$
Stage loss (with exit energy = stator + rotor loss + exit energy)	$\xi_{12c} = (h_{2T} - h_{2s'}) / (h_{0T} - h_{2s'})$

Tab. 1. Enthalpy losses in the stator, rotor and stage.

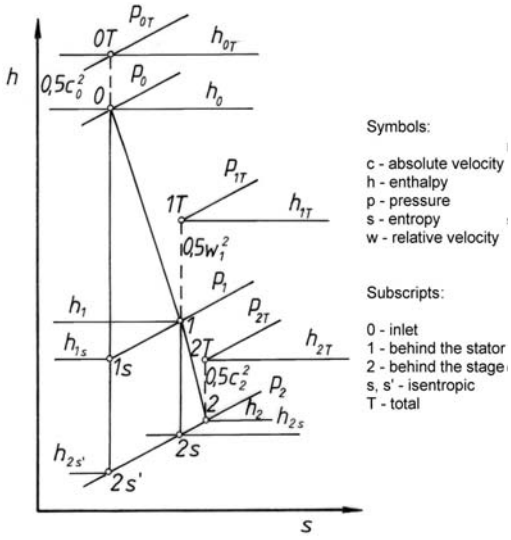

Fig. 10. Enthalpy-entropy diagram for a turbine stage